Bioorganic & Medicinal Chemistry Letters 30 (2020) 127492

Contents lists available at ScienceDirect

Bioorganic & Medicinal Chemistry Letters

journal homepage: www.elsevier.com/locate/bmcl

Synthesis and anti-cancer activity of bis-amino-phosphine ligand and its ruthenium(II) complexes

Zelinda Engelbrecht[a,b], Kim Elli Roberts[a,b], Ayesha Hussan[a], Gershon Amenuvor[c,d], Marianne Jaqueline Cronjé[b], James Darkwa[c], Banothile C.E. Makhubela[c], Lungile Sitole[a,*]

[a] Department of Biochemistry, University of Johannesburg, PO Box 524, Auckland Park, Johannesburg 2006, South Africa
[b] School of Molecular and Cell Biology, University of the Witwatersrand, Private Bag 3, Wits 2050, South Africa
[c] Research Centre for Synthesis and Catalysis, Department of Chemical Sciences, University of Johannesburg, Auckland Park, Johannesburg 2006, South Africa
[d] Council for Scientific and Industrial Research (CSIR) Institute of Industrial Research, PO Box LG 576, Accra, Ghana

ARTICLE INFO

Keywords:
Ruthenium(II)
Amino-phosphine
Anti-cancer
Melanoma and Piano-Stool

ABSTRACT

The development of both chemotherapeutic drug resistance as well as adverse side effects suggest that the current chemotherapeutic drugs remain ineffective in treating the various types of cancers. The development of new metallodrugs presenting anti-cancer activity is therefore needed. Ruthenium complexes have gained a great deal of interest due to their promising anti-tumour properties and reduced toxicity *in vivo*. This study highlighted the effective induction of cell death in a malignant melanoma cell by two novel bis-amino-phosphine ruthenium (II) complexes referred to as **GA105** and **GA113**. The IC_{50} concentrations were determined for both the complexes, the ligand and cisplatin, for comparison. Both complexes **GA105** and **GA113** displayed a high anti-cancer selectivity profile as they exhibited low IC_{50} values of 6.72 μM and 8.76 μM respectively, with low toxicity towards a non-malignant human cell line. The IC_{50} values obtained for both complexes were lower than that of cisplatin. The new complexes were more effective compared to the free ligand, **GA103** (IC_{50} = > 20 μM). Morphological studies on treated cells induced apoptotic features, which with further studies could indicate an intrinsic cell death pathway. Additionally, flow cytometric analysis revealed that the mode of cell death of complex **GA113** was apoptosis. The outcomes herein give further insight into the potential use of selected Ru(II) complexes as alternative chemotherapeutic drugs in the future.

Melanoma is an aggressive form of cancer and has an exceptionally high incidence rate worldwide, evident from the increase seen over the past 50 years. Modern therapeutics remain a challenge (high-priced cost and the unavailability of functioning equipment) in melanoma treatment.[1,2] Cytotoxic platinum-based chemotherapy is not so effective in targeting melanoma, as such the overall survival of melanoma patients is uncertain when compared to other cancer types. Alternative anti-cancer metallodrugs, which incorporate different transition metals from the platinum group series, such as ruthenium, need to be developed.[3]

Given the success of platinum-based therapies, interest in ruthenium complexes (which also share chemical similarity and comparable ligand exchange kinetics to platinum) has significantly increased. A large number of ruthenium compounds have sparked great interest due to their promising anti-tumour properties, particularly the leading complexes NAMI-A ((ImH)[trans-$RuCl_4$(dmso-S)(Im)], Im = imidazole), KP1019 ((IndH)[trans-$RuCl_4(Ind)_2$], Ind = indazole) and KP1339 (Na [trans-$RuCl_4(Ind)_2$])), all of which are currently in clinical trials.[4–6] In comparison to platinum, ruthenium complexes are said to have reduced toxicity and increased tolerability *in vivo*.[5,7] This is attributed to the fact that malignant cancerous cells over-express transferrin receptors due to their high demand for iron. The triad metals, such as ruthenium, are able to mimic iron in its binding to serum transferrin. In so doing, these ruthenium complexes are biologically tolerable and may be delivered more efficiently to the cancerous cells.[6,8,9] In addition, ruthenium complexes are known to typically adopt different oxidation states (II, III, and IV), assume an octahedral molecular geometry (pseudo octahedral in half-sandwich complex forms) and have a relatively slow rate of ligand exchange as compared to other transition metal complexes.[6,9] These characteristics have therefore made ruthenium-based complexes attractive anti-cancer candidates.[5,6,9] For instance, under certain biological circumstances (hypoxia, acidosis and increased glutathione), the less active and non-toxic ruthenium(III) complexes are activated by reduction to the active ruthenium(II) complexes which have been

* Corresponding author at: Department of Biochemistry, University of Johannesburg, PO Box 524, Auckland Park, Johannesburg 2006, South Africa.
E-mail address: lsitole@uj.ac.za (L. Sitole).

https://doi.org/10.1016/j.bmcl.2020.127492
Received 21 March 2020; Received in revised form 6 August 2020; Accepted 9 August 2020
Available online 11 August 2020
0960-894X/

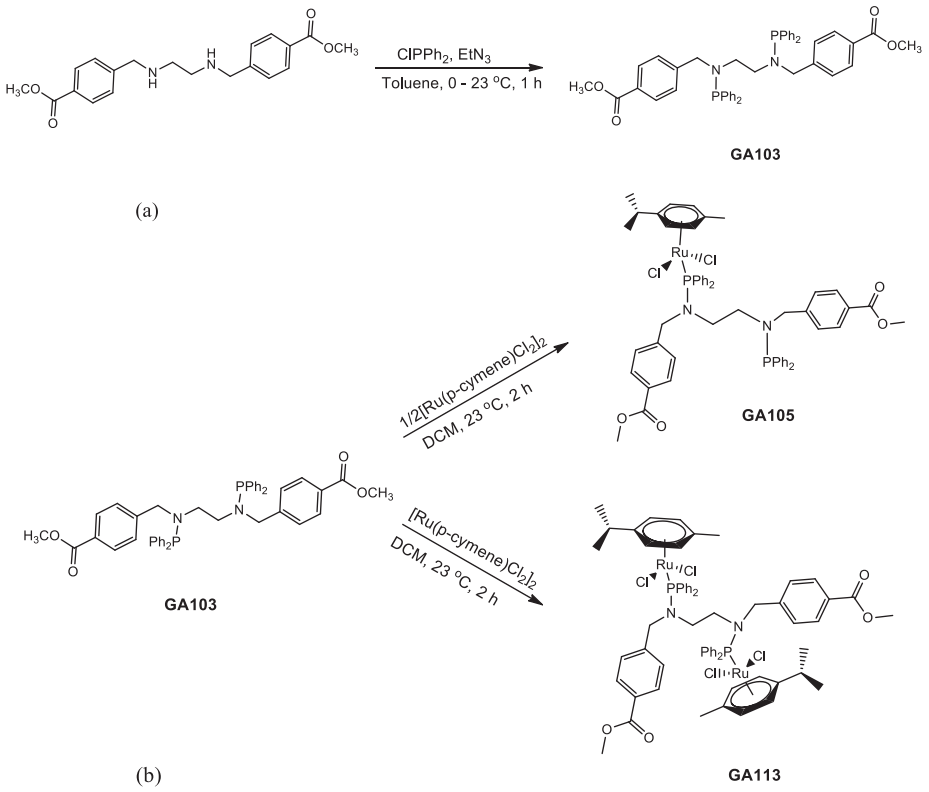

Scheme 1. Synthesis of ligand (a) **GA103** and complexes (b) **GA105** and **GA113**.

shown to directly kill cancerous cells.[5–7] Also, the slow ligand exchange rate of ruthenium-based complexes makes them suitable for biological use since their slow rates of ligand exchange are comparable to those of cellular processes.[5–7]

In recent years many research groups have explored the potential use of "piano-stool" ruthenium(II) arene complexes as chemotherapeutic agents based on the "activation by reduction" hypothesis.[5,6] One such example is NAMI-AR, which was obtained by reduction of NAMI-A[10]. In their study, Sava *et al.* showed that the reduced NAMI-AR was more efficient than NAMI-A in inhibiting metastatic cancerous growth.[10] In addition, other ruthenium(II) arene complexes such as [Ru (C_6H_6) (DMSO) Cl_2], RAPTA-C and KP1558 have also been shown to possess promising anti-cancer and anti-metastatic potential.[9]

Besides arene ligands, several other ligand types including phosphine, nitrogen and oxygen donor ligands have featured in the design of potential chemotherapeutic metallodrugs.[11] Some ligands that contain more than one donor atoms have been carefully designed with a reasonable spacer that can allow accommodation of two metal centres to form bimetallic compounds. Typical examples are the dinuclear bis-phosphino-amine ruthenium(II) complexes reported recently by Broomfield *et al.*[12]. Unlike the dinuclear platinum metallodrugs that have proven to retain activity even in cisplatin resistant cell lines,[13] the cytotoxicity of bimetallic ruthenium(II) arene compounds is a field significantly unexplored.[12,14] In the study reported by Broomfield *et al.*, bimetallic compounds containing a linker with two carbon atoms between the nitrogen atoms were more active compared with the compounds having a longer linker.[12] Findings from Broomfield *et al*, amongst others, support the need to investigate bimetallic compounds as potential anti-cancer chemotherapeutic agents.

Based on the promising biological activity of arene ruthenium(II) complexes having phosphorus moiety as an auxiliary ligand, we synthesized and characterized a novel bis-amino-phosphine ligand (**GA103**) and two of its corresponding ruthenium(II) complexes (referred to as **GA105** and **GA113**). These were screened for their anti-cancer activity against human melanoma cancer cells A375.

Synthesis of compounds

The bis-amino-phosphine ligand (**GA103**) specially designed to accommodate one or two ruthenium(II) centres *via* the phosphorus atoms in a monodentate fashion was synthesized following a protocol illustrated in Scheme 1**a**. The reaction of **GA103** with half mole equivalent of [Ru(*p*-cymene)Cl_2]$_2$ in dichloromethane afforded complex **GA105** (Scheme 1**b**) in a high yield of 96%. A monodentate bimetallic complex **GA113** was obtained in an excellent yield (> 99%) when one mole equivalent of the metal precursor was reacted with the ligand as shown in Scheme 1**a**. Both complexes were isolated as reddish-brown solids. The two complexes readily precipitated from *n*-hexane as pure products; and thus, did not need further purification.

Elemental analysis, mass spectrometry, ^{1}H NMR, ^{13}C{^{1}H} NMR and ^{31}P {^{1}H} NMR were used for the characterization of the complexes. The single crystal X-ray structure of **GA113** was determined, which revealed the characteristic "piano-stool" geometry at the ruthenium centres (Fig. S1, Supplementary information). The structure shows the η^6 π-bonded arene rings with the three other ligands on the metal ions. The crystallographic data and refinement parameters are listed in Table S1 (Supplementary Information). The Ru-P and Ru-Cl bond lengths for **GA113** (Table S1) are in the expected range found for similar ruthenium/diaminophosphine complexes.[11,12] The observed P—N bond length of 1.696 Å and the Ru—P—N bond angle of 116.24 are comparable to literature findings.[14]

Anti-cancer activities and morphological changes

The anti-cancer activity of various phosphine-based ruthenium complexes have previously been reported.[12,14–17] In this study, the anti-cancer ability of the phosphine-based complexes including the ligand were evaluated using an alamarBlue® proliferation assay for both malignant A375 and non-malignant HEK293 cells. This assay measures the mitochondrial activity which is directly proportional to the cell viability. The non-malignant HEK293 cells were used in order to identify

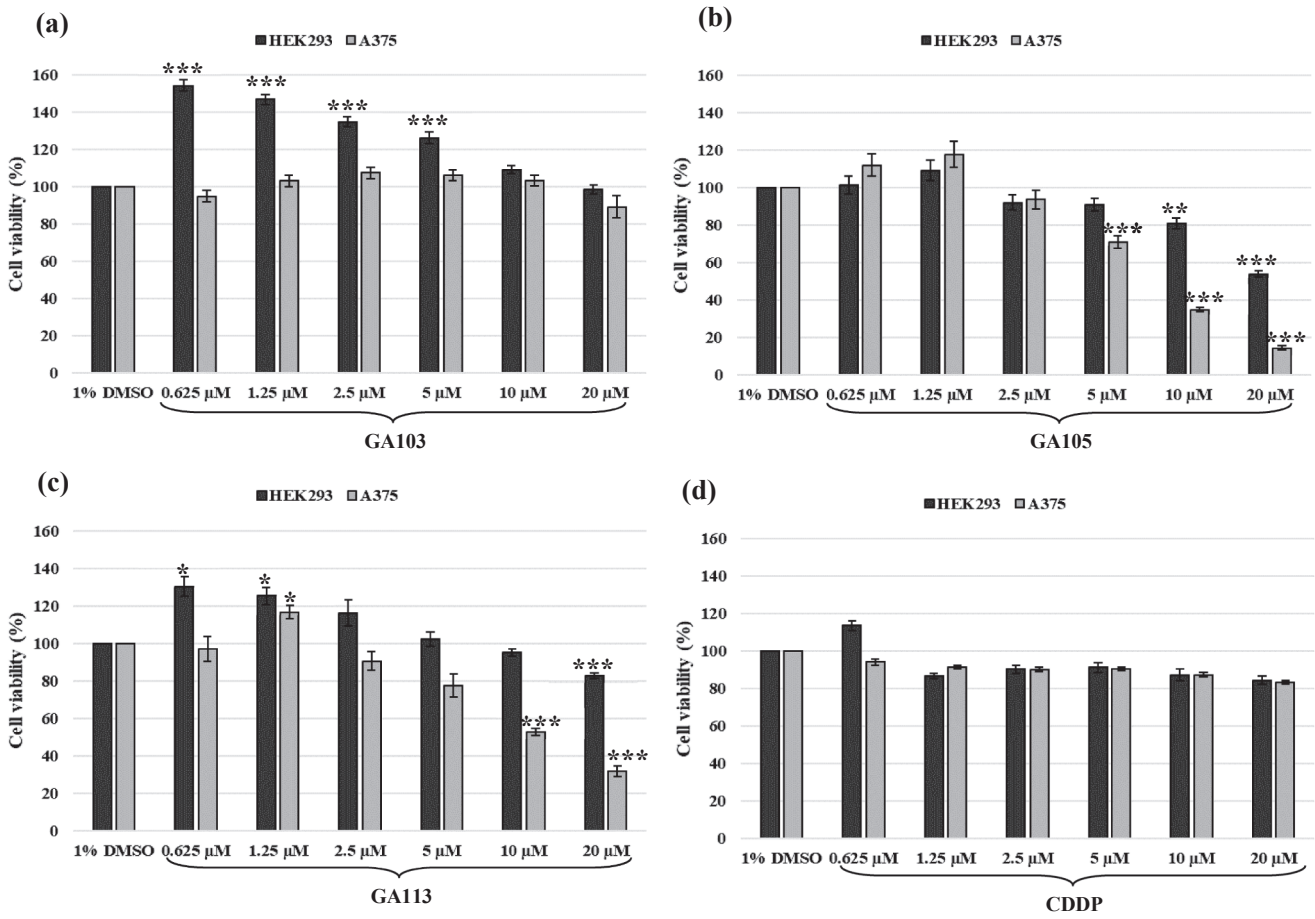

Fig. 1. The percentage cell viability of human non-malignant HEK293 (dark grey) and malignant A375 (light grey) cells analysed with an alamarBlue® proliferation assay. The cells were treated for 24 h with a concentration range of either (a) **GA103**, (b) **GA105**, or (c) **GA115** dissolved in DMSO (vehicle control). In addition, a positive control, (d) CDDP was also included at varying concentrations and compared to the treatments under study.

Table 1
Calculated IC_{50} concentrations for the different treatments in both non-malignant HEK293 and malignant A375 cells. The Standard deviation (± Std dev) is indicated and is representative of at least three independent experiments.

Cell line	HEK293	A375
IC_{50} concentrations/ ± Std dev		
GA103	> 20 µM	> 20 µM
GA105	14.30 µM (± 2.30 µM)	6.72 µM (± 2.02 µM)
GA113	> 20 µM	8.76 µM (± 1.37 µM)
CDDP	> 20 µM	> 20 µM

treatment that is selective for malignant cells without causing any harm to the non-malignant cells.

Dose-response graphs were constructed in order to determine the IC_{50} concentrations of the various treatments including cisplatin (CDDP) (Fig. 1). The effect of the ligand (**GA103**) on its own was evaluated on both cell lines. Overall, the ligand had minimal effect on both the cell lines with viabilities exceeding 90% (Fig. 1**a**). This comes as no surprise since most ligand and complex entities show higher anti-cancer activity when combined. For complexes **GA105** and **GA113**, a dose-dependent decrease in the cell viability was observed in the malignant A375 cells (Fig. 1**b** and **c**). Both complexes were less toxic to the non-malignant HEK293 cells. Overall, CDDP did not have any significant effect on either the HEK293 or A375 cells (Fig. 1**d**).

Following cell viability testing, the IC_{50} concentrations were determined for both the non-malignant and malignant cell models (Table 1).

For the HEK293 cells, the ligand (**GA103**), complex **GA113** and CDDP had IC_{50} values exceeding 20 µM. Furthermore, **GA103** and CDDP displayed IC_{50} values higher than 20 µM in the A375 cells. Complex **GA105** had the lowest IC_{50} value (6.72 µM) in the malignant A375 cells when compared to **GA113** (8.76 µM), however it was the less selective in comparison to **GA113** in the HEK293 cells (14.30 µM vs > 20 µM). In a study done by Aliende *et al.* [16a] a series of ruthenium complexes containing either 2-(diphenylphosphino)-1-methylimidazole or diphenyl-2-pyridylphosphine were tested for anti-cancer activity in breast and pancreatic cancer cell models. The complexes displayed IC_{50} values ranging from 3.3 to 62 µM for the breast and 6.6–35.33 µM for the pancreatic cancer cells after 48hr of treatment.[16] Ruthenium(II) arene complexes coordinated to a series of ligands, that include 1, 3, 5-triaza-7-phosphaadamantane (PTA), have also been shown to target human ovarian carcinoma cell lines that are either resistant or non-resistant to CDDP.[18] In their study Pettinari *et al.*, observed that the PTA containing complexes displayed a high selectivity profile as they were more toxic to the malignant cells (0.14–1.18 µM) than the non-malignant HEK293 cells (2–30 µM) after 72 h of exposure.[18] Findings from our study are therefore in agreement with previous literature observations indicating the toxicity of ruthenium complexes on malignant cell lines.

To further investigate the anti-cancer effect, morphological studies were conducted only for the malignant A375 cells. Three concentrations (5, 10 and 20 µM) were chosen and are depicted in Fig. 2. These concentrations were chosen based on the IC_{50} range (5 µM–20 µM) where cellular inhibition occurred. The DMSO-treated cells appeared confluent and intact (Fig. 2**a**). Meaning, DMSO had no effect on cellular

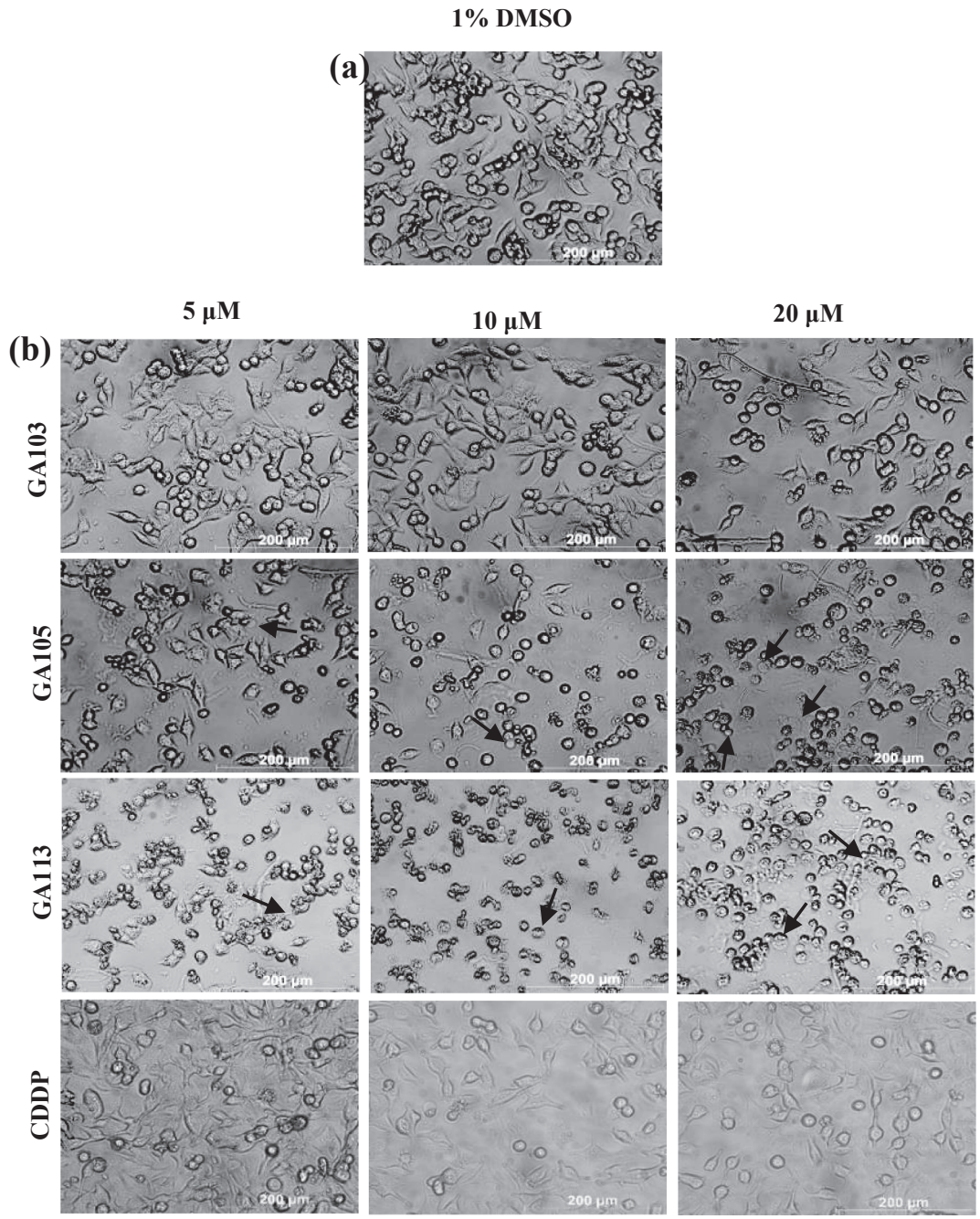

Fig. 2. Morphological studies of A375 melanoma cancer cells after being exposed to the (a) vehicle control (DMSO) and (b) three concentrations (5, 10 and 20 µM) of **GA103**, **GA105**, **GA113** and CDDP. Images were captured after 24 h of treatment at a magnification of 200x using an inverted light microscope (n = 3). Signs of cellular rounding and membrane blebbing are highlighted with the black arrows.

viability. For the **GA103** and CDDP-treated cells, a similar morphology was observed for all three concentrations (Fig. 2**b**). The cellular morphology for both complexes was analysed using light microscope and was seen to be consistent with apoptotic features such as chromatin condensation, cell shrinkage and a decrease in the number of viable cells.

Apoptosis is an orderly process and can be divided into two pathways, the mitochondrial-mediated pathway and the death receptor pathway, both of which are controlled by apoptotic-related proteins, well-known as caspases.[19] For both the **GA105** and **GA113**-treated cells, the cells appeared to be less confluent and the morphology changed as the concentration increased (Fig. 2**b**). The cells appeared more rounded and some characteristics of membrane blebbing (as indicated by the black arrows) could be observed, which is unique to apoptotic cell death.[20] Taken together, the morphological changes observed in this study indicate that complexes **GA105** and **GA113** could trigger apoptotic cell death. Previous studies have confirmed apoptotic cell death by apoptosis-associated ccaspase activation assays.[20–22] For instance, in a study done by Bomfim *et al.*, ruthenium(II) complexes with 6-methyl-2-thiouracil (6m2tu) *cis*-[Ru(6m2tu)$_2$(PPh$_3$)$_2$] and [Ru(6m2tu)$_2$(dppb)] induced caspase-mediated apoptosis in myeloid leukaemia cell lines.[21]

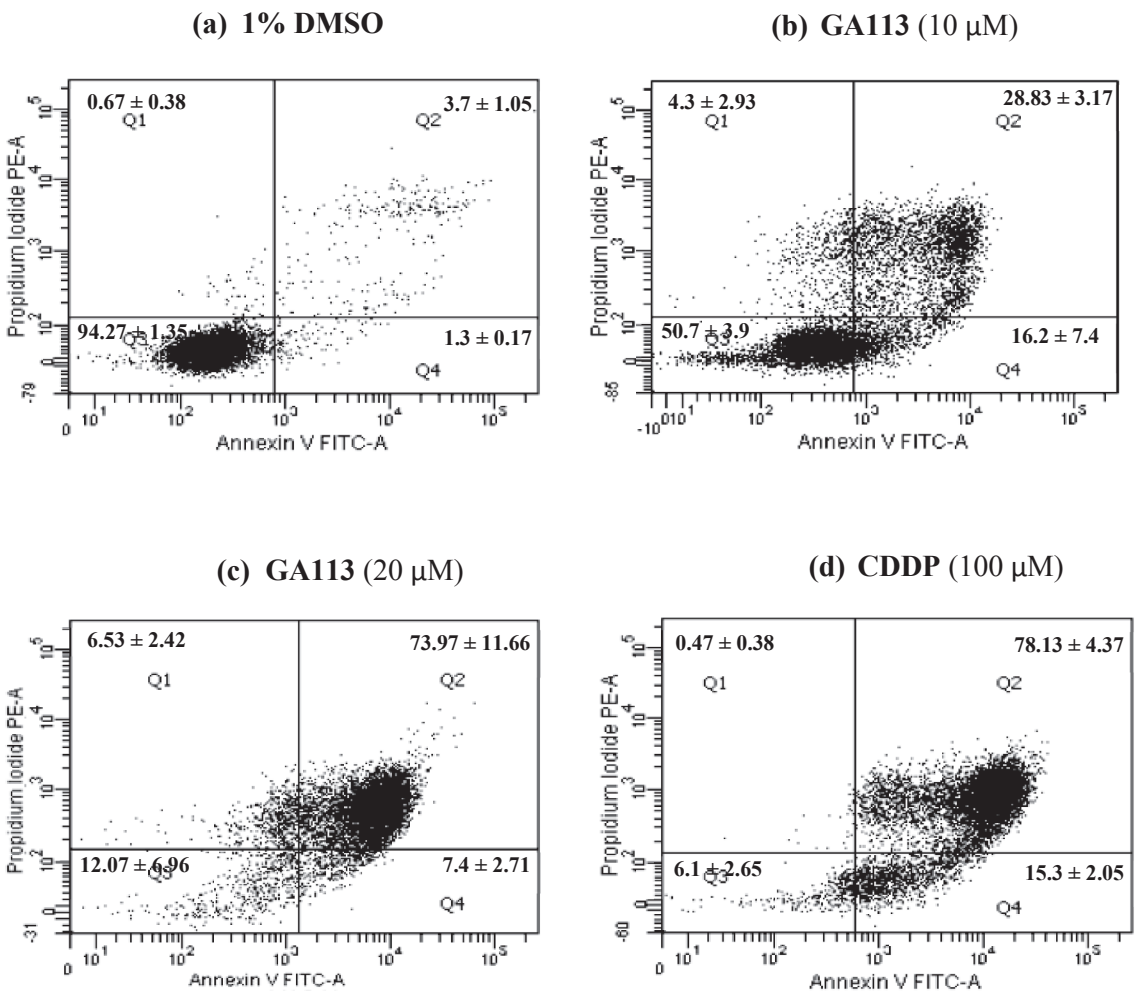

Fig. 3. Mode of cell death in A375 malignant cells stained with FITC-Annexin V/PI. Representative flow cytometry dot plots are presented in: (a) 1% DMSO (vehicle control) treatment, (b) treated with 10 μM **GA113** (d) treated with 20 μM **GA113** and (e) 100 μM CDDP (positive apoptotic control for 24 h. Quadrant 1 (Q1) = necrosis; quadrant 2 (Q2) = late apoptotic phase; quadrant 3 (Q3) = viable cells and quadrant 4 (Q4) = early apoptotic phase.

Confirmation of cell death

To confirm that the complexes induced apoptosis in the malignant A375 cells, as predicted in the morphological studies, the mode of cell death was investigated using FITC-Annexin-V/PI labels in flow cytometry. For this specific assay, only **GA113** was tested because of its low toxicity to HEK293 non-malignant cells as well as its high selective anti-cancer profile as compared to **GA105**. The flow cytometry assay exploits the exposure of phosphatidylserine (PS) protein, an event that only occurs in apoptosis. The four quadrants in the dot plots (Fig. 3) are designated as Q3 which represent viable cells, Q4 and Q2 represent early and late apoptotic cells respectively and Q1 represents necrotic cells. The DMSO-treated cells (Fig. 3**a**) were mostly located in Q3, the viable quadrant, with a percentage cell population of 94.27%. Cells for the apoptotic control, 100 μM CDDP (Fig. 3**d**), were mostly located in quadrants Q4 and Q2, the apoptotic quadrants. The combined apoptotic cell population was 93.43%. In cells treated with 10 μM of **GA113** (Fig. 3**b**) 16.2% were in early apoptosis (Q4) and 28.83% of cells were in late apoptosis (Q2), with minimal cells located in the necrotic quadrant Q1. The combined early and late apoptotic populations were 45.03%. In cells treated with 20 μM **GA113** (Fig. 3**c**), most of the cell population were located in the late apoptotic quadrant Q2, with a percentage of 73.97%. Q4, the early apoptosis quadrant had 7.4% of cells, bringing the total apoptotic population in 20 μM **GA113** treated cells to 81.37%.

Considering that cells treated with complex **GA113** were detected in the apoptotic quadrants in flow cytometry (Fig. 3**b and d**) and together with the morphological apoptotic features observed in Fig. 2, it is evident that the mode of cell death of **GA113**, is apoptosis. Similar findings in other studies have also reported the mode of cell death as apoptosis for various phosphine-based ruthenium(II) complexes. For instance, a study reported by Lima *et al.* investigated a phosphine-based ruthenium complex, $[Ru(gly)(bipy)(dppb)]PF_6$, which induced apoptosis in sarcoma cells determined by flow cytometry in addition to other apoptotic assays.[23] Additional studies are required to determine the type of apoptosis mediated by the complex. Overall, results obtained from this study suggest ruthenium complexes possess potential as anti-cancer agents.

In conclusion, two novel arene ruthenium(II) complexes bis-phosphino-amine ligand were synthesized, characterized and tested for anti-cancer potential against a malignant melanoma cell line as well as a non-malignant cell line. **GA113** displayed a highly selective anti-cancer profile as it hindered cellular proliferation in malignant A375 melanoma cells and not that of non-malignant HEK293 cells. Complex **GA113** also inhibited the growth of A375 malignant cells by inducing apoptosis. Such a complex could possess potential as an alternative targeted chemotherapeutic agent.

The findings of this study should however be seen in light of some limitations. For instance, the experimental conditions, for the biological evaluation, may have led to changes in the chemical structure of

GA113. The fact that stability studies to confirm that the structure of **GA113** was not affected by the experimental conditions, were not performed, is a study limitation. Future studies will therefore focus on stability testing, quantitative confirmation of apoptotic induction, syntheses of more and similar derivatives as well as structure-activity relationship studies between ligand and complex. Additionally, aqueous solubility evaluation between **GA113** and cisplatin should be investigated in order to appraise the possible administration methods for **GA113** for both *in vitro* and future *in vivo* studies. Upon further investigation, these findings will aid in the development of new drug candidates that function as anti-cancer inhibitors.

Declaration of Competing Interest

The authors declare that they have no known competing financial interests or personal relationships that could have appeared to influence the work reported in this paper.

Acknowledgements

The authors gratefully acknowlege financial assistance from the University of Johannesburg. This work is based on the research supported in part by the National Research Foundation (Thutuka) of South Africa with grant ID number: TTK70515230989.

Appendix A. Supplementary data

Crystallographic data (excluding structure factors) for the structure (**GA113**) in this paper has been deposited with the Cambridge Crystallographic Data Centre as supplementary publication no. CCDC 1986020. Supplementary data to this article can be found online at https://doi.org/10.1016/j.bmcl.2020.127492.

References

1. Meyle KD, Guldberg P. *J Hum Genet.* 2009;126:499–510.
2. Luo C. *J Cancer Lett.* 2017;397:120–126.
3. Gold M, Mujahid Y, Ahmed K, et al. *J Biol Inorg Chem.* 2019;24:647–657.
4. Antonarakis ES, Emadi A. *Cancer Chemother Pharmacol.* 2010;66(1):1–9.
5. Coverdale JPC, Laroiya-McCarron T, Romero-Canelón I. *Inorganics.* 2019;7:1–15.
6. Süss-Fink G. *Dalton Trans.* 2010;39:1673–1688.
7. Lin K, Zhao ZZ, Bo H, Hao XJ, Wang JQ. *Front Pharmacol.* 2018;9:1–10.
8. Iida J, Bell-Loncella ET, Purazo ML, et al. *Transl Med.* 2016;14:1–10.
9. Motswainyana WM, Ajibade PA. *Adv Chem.* 2015:1–21.
10. Sava G, Bergamo A, Zorzet S, et al. *Eur J Cancer.* 2002;28:427–435.
11. (a) Representative recent examples of various types of ligands for metallodrug design: Samper KG, Marker SC, Bayón P, et al. *J Inorg Biochem.* 2017;174:102–110
(b) Agonigi G, Riedel T, Zacchini S, Păunescu E, et al. *Inorg Chem.* 2015;54:6504–6512
(c) Aznar R, Grabulosa A, Mannu A, Muller G, Sainz D, et al. *Organometallics.* 2013;32:2344–2362
(d) Ludwig G, Kaluderovic GN, Ruffer T, Bette M, Korb M, et al. *Dalton Trans.* 2013;42:3771–3774
(e) Paschke H, Langc, Steinborn D. *Dalton Trans.* 2013;42:3771–3774
(f) Mei C. *Biomaterials.* 2017;129:111–126
(g) Haghdoost M, Golbaghi G, Létourneau M, Patten SA, Castonguay A. *Eur J Med Chem.* 2017;132:282–293
(h) Basri AM, Lord RM, Allison SJ, Rodríguez-Bárzano A, Lucas SJ, Janeway FD, et al. *Chem Eur J.* 2017;23:6341–6356
(i) Rono CK, Chu WK, Darkwa J, Meyer D, Makhubela BCE. *Organometallics.* 2019;38:3197–3211
(j) Matsheku AC, Chen MYH, Jordaan S, Prince S, Smith GS, Makhubela BCE. *Appl Organomet Chem.* 2017;31:3852–3865
(k) Crochet P, Gimeno J, Borge J, García-Granda S. *New J Chem.* 2003;27:414–420.
12. Broomfield LM, Alonso-Moreno C, Martin E, et al. *Dalton Trans.* 2017;46:16113–16125.
13. Ruhayel RA, Langner JS, Oke M-J, Berners-Price SJ, Zgani I, Farrell NP. *J Am Chem Soc.* 2012;134:7135–7146.
14. (a) Murray BS, Menin L, Scopelliti R, Dyson PJ. *Chem Sci.* 2014;5:2536–2545
(b) Saeed HK, Saeed IQ, Buurma NJ, Thomas JA. *Chem Eur J.* 2017;23:5467–5477
(c) Magennis SW, Habtemariam A, Novakova O, Henry JB, Meier S, et al. *Inorg Chem.* 2007;46:5059–5068
(d) Mendoza-Ferri M-G, Hartinger CG, Eichinger RE, Stolyarova N, et al. *Organometallics.* 2008;27:2405–2407
(e) Mendoza-Ferri M-G, Hartinger CG, Mendoza MA, Groessl M, Egger AE, Eichinger RE, Mangrum JB, Farrell NP, Maruszak M, Bednarski PJ, Klein F, et al. *J Med Chem.* 2009;52:916–925
(f) Stringer T, Therrien B, Hendricks DT, Guzgay H, Smith GS. *Inorg Chem Commun.* 2011;14:956–960
(g) Gras M, Therrien B, Süss-Fink G, Zavab O, Dyson PJ. *Dalton Trans.* 2010;39:10305–10313
(h) Priya S, Balakrishna M, Mobin S, McDonald R. *J Organomettalic Chem.* 2003;688:227–235
(i) Amenuvor G, Rono CK, Darkwa J, Makhubela BCE. *Eur J Inorg Chem.* 2019:3942–3953.
15. (a) Popolin CP, Reis JPB, Becceneri AB, et al. *PLoS ONE.* 2017;12:1–21
(b) Amenuvor G, Makhubela BCE, Darkwa J. *Catal Sci Technol.* 2018;8:2370–2380
(c) Amenuvor G, Makhubela BCE, Darkwa J. *ACS Sustainable Chem Eng.* 2016;4:6010–6018
(c) Biancalana L, Pampaloni G, Marchetti F, Chimia. *Int J Chem.* 2017;71(9):573–579.
16. Aliende C, Pérez-Manrique M, Jalón FA, et al. *J Inorg Biochem.* 2012;117:171–188.
17. Pettinari R, Marchetti F, Condello F, et al. *Organometallics.* 2014;33(14):3709–3715.
18. Sánchez VC, Nieto-Jiménez C, Castro-Osma JA, et al. *ACS Omega.* 2019;4(8):13005.
19. Deng Z, Gao P, Yu L, et al. *Biometals.* 2017;129:111–126.
20. Jiang G, Zhang W, He M, et al. *Polyhedron.* 2019;169:209–218.
21. Bomfin LM, de Araujo FA, Dias RB, et al. *Nature.* 2019;9(11483):1–17.
22. Chen J, Zhang Y, Li G, et al. *J Biol Inorg Chem.* 2018;23:261–275.
23. Lima AP, Pereira FC, Almeida MAP, et al. *PLoS ONE.* 2014;9:1–11.